Combining Electrical Measurements and Mercury Porosimetry to Predict Permeability

Douglas Ruth, Professor and Dean Emeritus, Faculty of Engineering, University of Manitoba

Craig Lindsay, Director, Core Specialist Services

Mark Allen, Lead Reservoir Engineer West Africa, Tullow Oil PLC

This paper was prepared for presentation at the International Symposium of the Society of Core Analysts held in Aberdeen, Scotland, UK, 27-30 August, 2012

ABSTRACT

From the 1940s through the 1980s, the work of such researchers as Purcell, Leverett, Swanson, and Thomeer provided methods for predicting flow properties, particularly permeability, based on capillary pressure curves measured on rock-mercury-vacuum systems. Although these methods met with considerable success, they have been largely overshadowed, particularly in recent years, by the rapid development of network and direct models. This paper reports on a study of 24 samples from an Offshore Ghana formation of Turonian age. The paper demonstrates that the work of Purcell, in particular, can be used to provide primary predictions of permeability (that is, predictions without any flexible fitting parameters) provided that mercury porosimetry and formation factor measurements are available, either on identical or companion samples. The predictions are good to within a range of factors between 0.5 and 2, with a mean error of less than 35%. This accuracy is remarkable considering that the range of permeability is 7 decades and that the data was not collected for the specific purpose of the study. An experimental protocol is suggested that should improve further the already excellent results. The applicability of the method to drill cuttings is discussed. Also, a suggestion for a method of applying the proposed technique to digital rock results is presented. Finally, the paper explores reasons behind the success of the predictions and suggestions what types of reservoirs are expected to provide similar successes.

INTRODUCTION

Introduction of mercury injection porosimetry (MIP) in 1945 by Drake and Ritter[1] provided a simple and quick method of exploring the structure of porous media. Methods based on the shape of the MIP curves and on the integration of these curves have subsequently been developed in order to predict transport properties including permeability and relative permeability (Leverett[2], Purcel[3], Thomeer[4], Swanson[5]). Most of these methods were based on the assumption that the fluids acted as if flowing in a set of parallel capillary tubes. The current paper makes similar arguments but uses a representative elemental volume approach.

THE REPRESENTATIVE ELEMENTAL VOLUME MODEL

Single component flow through a porous media, regardless of how complex that media may be, can always be modeled as flow through a series of identical representative elemental volumes (REV) that contain a single tortuous tube, provided that the length and diameter of this tube is selected appropriately. This is a simple application of effective medium theory. Such an REV is illustrated in Figure 1. The total length of the tube is *L*, not equal to the bulk length L_b.

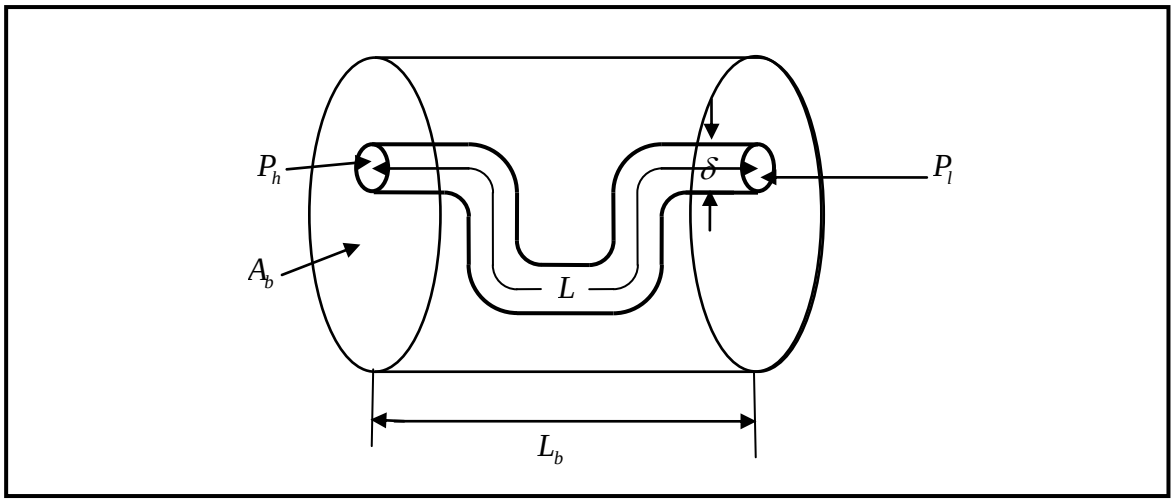

Figure 1 The model Representative Elemental Volume (REV)

The demonstration that this tube may be used to model a complex porous media proceeds as follows. The volumetric flow through the REV may be calculated from the equation

$$q = \frac{\pi\,\delta^4}{128\,\mu\,L}\,(P_a - P_b) \tag{1}$$

where μ is the viscosity and the other variables are defined in Figure 1. If the Darcy law is applied to this REV, the volumetric flow rate can be calculated from the equation

$$q = \frac{k\,A_b}{\mu\,L_b}\,(P_a - P_b) \tag{2}$$

where k is the permeability. Combining these equations, the permeability of the REV is given by

$$k = \frac{\pi\,\delta^4}{128\,A_b}\frac{L_b}{L} \tag{3}$$

The porosity, ϕ, of the REV is given by:

$$\phi = \frac{\pi\,\delta^2}{4\,A_b}\frac{L}{L_b} \tag{4}$$

and the tortuosity, τ, by:

$$\tau = \frac{L}{L_b} \tag{5}$$

Equations 3 through 5 may be combined to yield

$$k = \frac{\phi\, \delta^2}{32\, \tau^2} \tag{6}$$

If the rock is modelled as a homogeneous sample made up of REVs that look like this cell, the permeability may be predicted provided that appropriate estimates of the mean tube diameter and tortuosity are made.

The relation between the capillary pressure,P_c, in a tube and the tube diameter is

$$P_c = \frac{4\, \sigma \cos\theta}{\delta} \tag{7}$$

where σ is the interfacial tension and θ is the contact angle. Following the ideas put forward by Purcell, a mean value for the square of the tube size may be found from

$$\delta^2 = (4\, \sigma \cos\theta)^2 \int_0^1 \frac{dS_v}{(P_c)^2} \tag{8}$$

where S_v is the saturation of the vacuum in the MIP experiment. It follows that

$$k = \frac{\phi\, (\sigma \cos\theta)^2}{2\, \tau^2} \int \frac{dS_v}{(P_c)^2} \tag{9}$$

Although derived using a slightly different argument, this is Purcell's equation. However, the present derivation does not rely on the argument of parallel non-communicating tubes – it is in essence an effective medium theory.

By similar arguments to those above, the formation factor for the REV may be written as

$$F = \frac{4A_b}{\pi\, \delta^2} \frac{L_b}{L} \tag{10}$$

Using the porosity equation for this model (Equation 4), Equation 10 may be written as

$$F = \frac{\tau^2}{\phi} \tag{11}$$

If electrical properties are known for the plug then the permeability may be calculated from the equation

$$k = \frac{(\sigma \cos\theta)^2}{2\, F} \int \frac{dS_v}{(P_c)^2} \tag{12}$$

This equation gives a permeability prediction for a sample provided MIP and electrical properties are measured on the sample.

There will be many cases where the electrical properties are not available for the MIP samples but electrical measurements are available for samples from the same formation. In these cases, the tortuosity may be found from the Archie equation

$$F = \frac{a}{\phi^m} \tag{13}$$

where a and m are found by correlation of experimental results. Combining Equations 11 and 13 results in the following equation for tortuosity

$$\tau^2 = \frac{a}{\phi^{m-1}} \quad 14$$

It follows that the expression for permeability is

$$k = \frac{\phi^m (\sigma \cos\theta)^2}{2\,a} \int \frac{dS_v}{(P_c)^2} \quad 15$$

Because m is often approximated by 2 and a by 1, an expression for permeability in the complete absence of electrical data is

$$k = \frac{\phi^2 (\sigma \cos\theta)^2}{2} \int \frac{dS_v}{(P_c)^2} \quad 16$$

THE DATA SET

The data that form the basis of the present paper are from an offshore Ghana reservoir of Turonian age. The original core analysis test program was not designed especially for the present study – this study was conducted on an existing data set. To date, this data set has been used by the operator to populate permeability-porosity transforms and, supplemented by drill stem tests, to calibrate effective flow properties. In addition, reservoir models have been constructed in Petrel® and used to screen various field development options. The samples come from three different pools, one which produces oil and two which produce gas condensate.

There were 24 samples with MIP curves available (there was one additional sample but it not considered because the results were considered to be unreliable). Of these, two had electrical properties for the same sample. However, an additional 35 samples had permeability, porosity and formation factor measurements reported. Optimally, a study such as the present should use data collected on the same samples. Such data sets are not common but the present results should encourage more operators to collect them.

The MIP data was acquired using a Micromeritics Autopore IV. Permeability was measured at 3600 psi net overburden using a Core Lab CMS300 instrument. Formation factor was also measured at net overburden (3600 psi).

Figure 2 (Figures 2 through 6 are collected at the end of the paper) shows a composite plot of the MIP curves for the samples. It is well known that MIP curves can be interpreted in terms of pore throat size distributions. In the present work, pore throat size distributions are used as a surrogate for the tube sizes in the model derived above. Before the capillary pressure curves were used to determine mean pore throat diameters, they were corrected for surface pore invasion which is characterized by the small droop in the

curve near the vacuum-saturation-equals-unity axis. This correction is done by extrapolating the straight portion of the curve. The point where this extrapolation crosses the vacuum-saturation-equals-unity axis is the threshold capillary pressure. All points with capillary pressures less than the threshold pressure were removed and the saturation was scaled accordingly. The curves were then scaled with the threshold capillary pressure to obtain Figure 3.

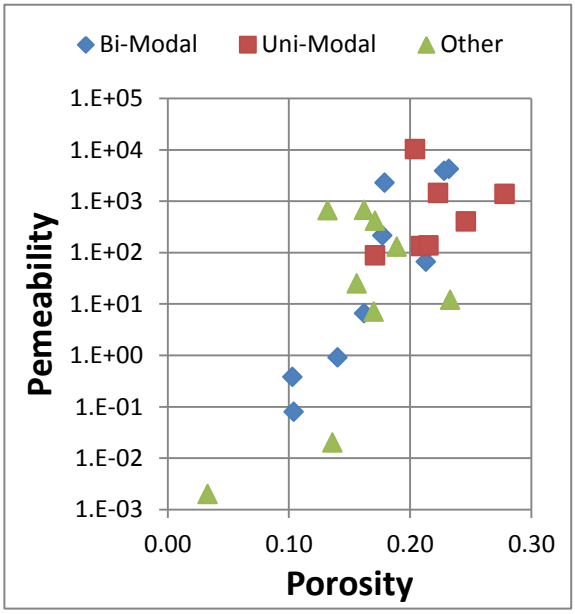

Figure 7 The -permeability/porosity crossplot.

A detailed analysis shows that there are similarities between various groups of curves. Figure 4 shows similarities for curves that appear to overlap each other and also show a bi-modal pore throat size distribution, caused by the presence of micro-porosity. Figure 5 shows similarities in curves that appear to overlap each other and also show a uni-modal pore throat size distribution. Finally, Figure 6 shows the remaining curves. This last set of curves shows differing types of pore throat size distributions including uni-modal and bi-modal types (a rather unique type is shown) and do not appear to overlap with the other sets of curves. Figure 7 shows a plot of the logarithm of permeability versus porosity differentiated by the "type" of the curve. Although there appears to be a trend between permeability and porosity and the curve types exhibit different behaviours, there is no obvious correlation evident, with permeability often varying by three to five orders of magnitude for the same porosity.

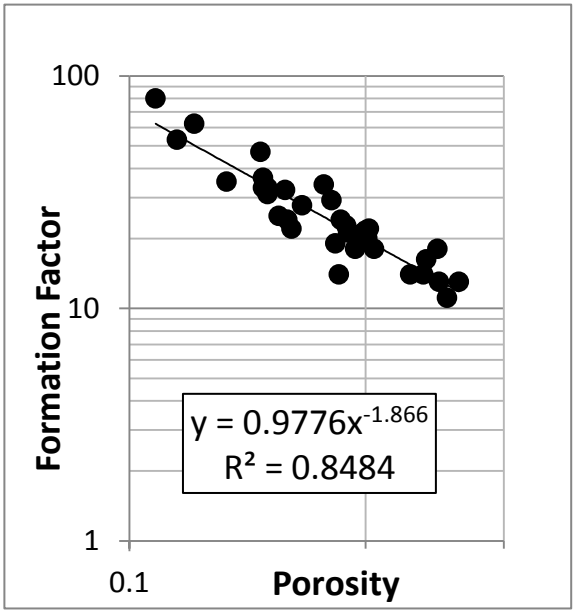

Figure 8 The formation factor/porosity crossplot.

Figure 8 shows the results for the electrical tests on the reservoir. The results were correlated using the Archie equation (Equation 13). The resulting values of the fitting parameters are $a = 0.9976$ and $m = 1.866$. The fit is not particularly good but the values of the fitting parameters are not much different from the Archie values of 1 and 2.

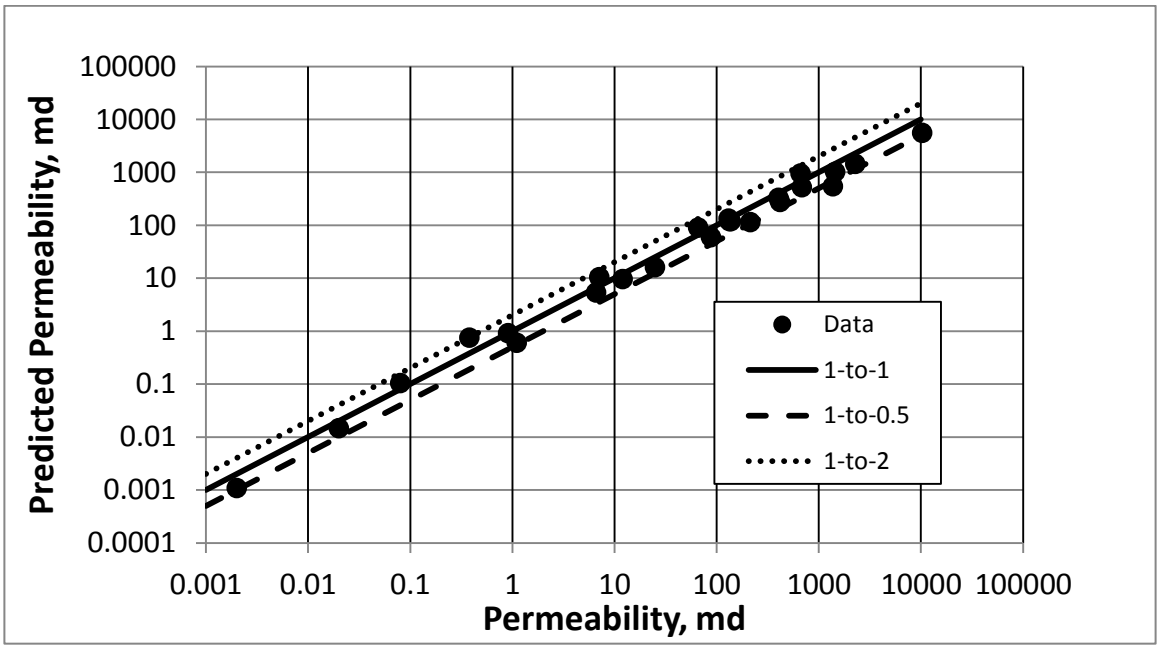

Figure 9 Comparison between the calculated permeability and the measured permeability using the formation factor correlation depicted in Figure 8.

The permeabilties were calculated from Equation 15 using the fitting electrical parameters found in this study. For these calculations, the values $\sigma = 480\ dyn/cm$ and $\theta = 140°$ were used. The integrals were performed using a simple numerical scheme. The results are shown in Figure 9 where the predicted permeability is compared with the measured permeability. Also plotted is a 1-to-1 correspondence line and two lines that indicate factor-of-two predictions (values which are twice as large and half as large as the measured permeability). The results are remarkable. Over a permeability range of almost seven decades, there is only one point that lies outside of the factor-of-two range. On average, the model under-predicts the values by about 13% and shows an absolute average disagreement of about 34%. Further, the model over-predicts 6 of the values and under-predicts 18 of the values.

It is of interest to determine how these results would change if the electrical measurements were not available and the original Archie model values are used (1 and 2 for a and m). This case is illustrated in Figure 10. The disagreement has increased with

considerably more cases of under-prediction. For this case, only 3 samples are over-predicted, the mean error is approximately 34% and the absolute average error is approximately 40%.

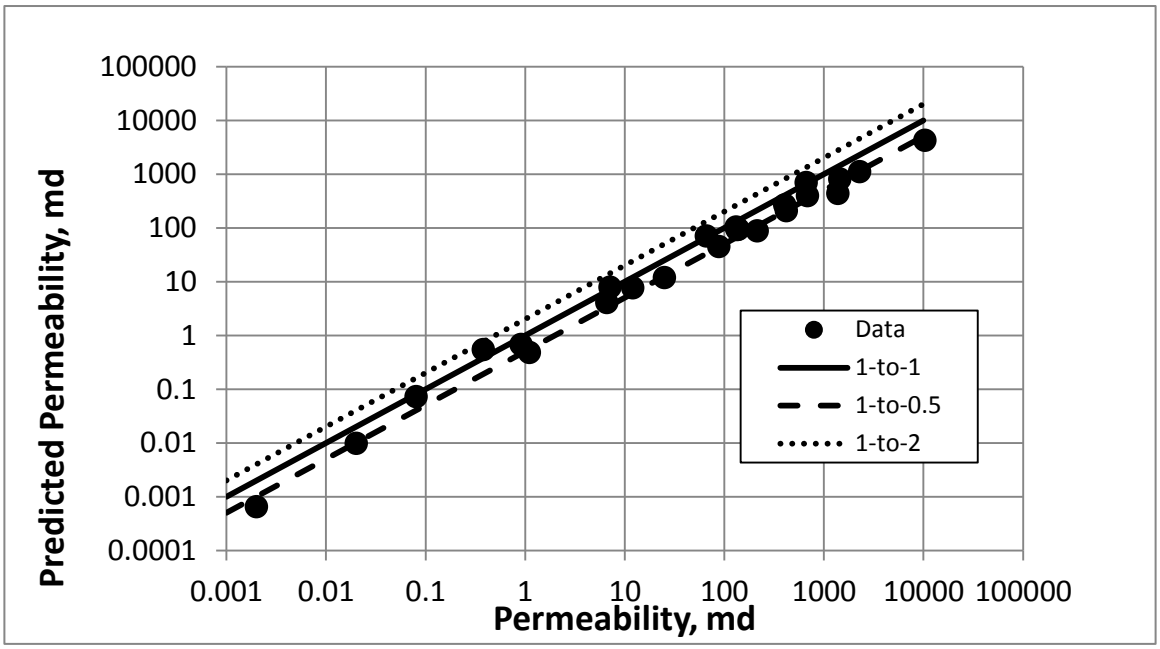

Figure 10 Comparison between the calculated permeability and the measured permeability using the Archie correlation ($a = 1$, $m = 2$).

APPLICATION TO DIGITAL ROCK TECHNIQUES

Current methods of investigating the pore structure of rocks using x-ray and magnetic resonance techniques have allowed detailed determination of pore sizes. These data are normally used to calculate flow properties by directly simulating the passage of fluids through the pore space. However, these data can also be used to generate synthetic capillary pressure curves or directly to calculate mean pore sizes. Such calculations are much simpler then flow calculations. Once these curves are available, the present work provides a simple and quick method to predict the permeability from these derived pore size distributions. This provides a means of checking the accuracy of the more complex simulated flow calculations that are currently used to predict permeability.

AN EXPERIMENTAL PROTOCOL

The present work is based on an existing data set, not originally intended to produce a predictive model for permeability. Despite this, a very accurate predictive tool was derived. In order to optimize this method, the following experimental protocol is suggested:

1. A core or series of cores representative of the full variability of the field should be obtained.
2. A detailed geological examination of the core should be performed in order to identify all the unique features of each facies of the field.
3. Twin samples should be taken from each of the identified unique features.
4. The permeability, porosity, and formation factor should be measured on all samples.
5. Mercury injection porosimetry should be performed on half of the duplicate samples, retaining the other half for data verification if necessary.
6. The Archie model should be determined by fitting the formation factor data.
7. The resulting permeability model should be tested to determine its applicability.

Once the model is verified, it can be used as a basis to determine the permeability in wells that are not cored. To make use of the correlation, electrical logs must be available (as is the usual case). The less common information is MIP results performed on drill cuttings. Such tests on drill cuttings are by no means routine. However, given the excellent results obtained in this study, MIP tests on drill cuttings (taking proper account of size effects on MIP experiments) may be a preferred way to obtain information on permeability in new wells. When combined with drill stem tests, a very complete picture of the flow behaviour of the reservoir may be possible.

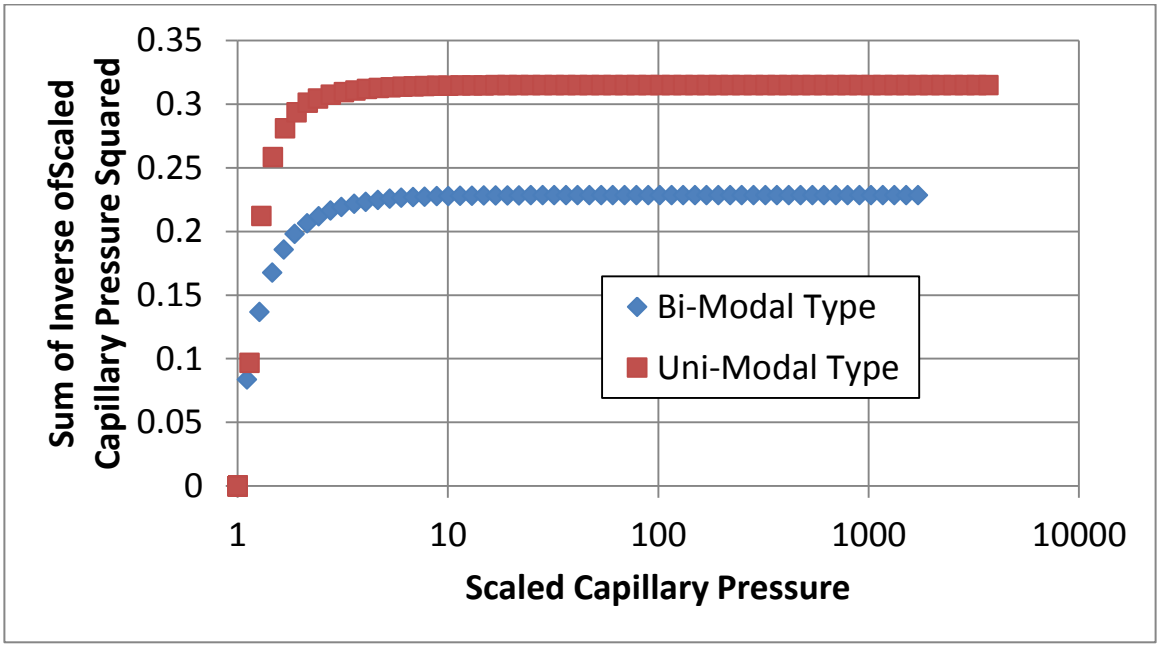

Figure 11 The progressive summation of the square of the inverse of the scaled capillary pressure. Only the largest tubes (lowest capillary pressures) play any role in the calculation of the permeability.

WHY DOES THE METHOD WORK SO WELL?

The reason that this method works so well may be understood by examining Figure 11. Here the progressive summation of the inverse of the square of the scaled capillary pressure is plotted against the scaled capillary pressure. This graph is a surrogate for a plot of the progressive calculation of the weighted mean square of the pore throat diameter plotted against the pore diameter. The plot begins at the threshold pressure (the scaled threshold pressure is unity). Clearly, only values of the scaled capillary pressure less than 10 have any impact on the weighted mean square of the pore diameter. It follows that the smaller pores play no role what-so-ever in the determination of the permeability and all that need be considered are the largest pores, at least in the case of the rocks examined in the present study. It follows that small pores, and particularly micro-porosity, play no role in controlling permeability for the current test samples.

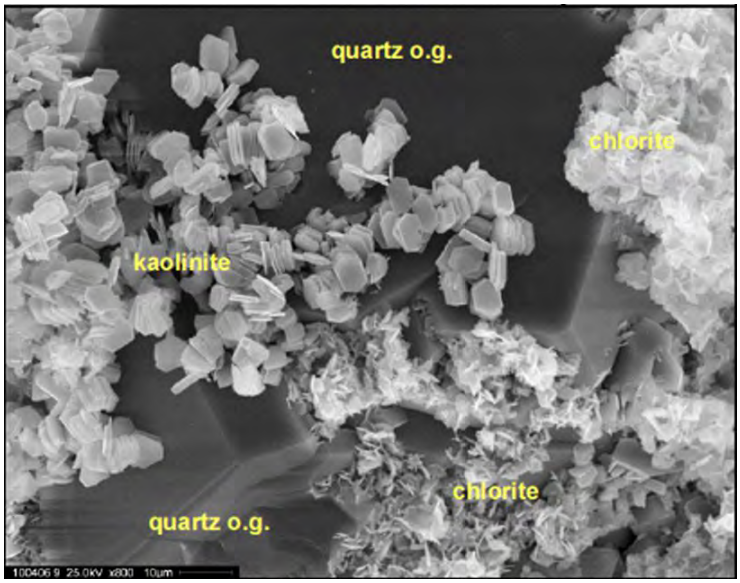

Figure 12 An SEM image of a typical sample showing the presence of moveable fines.

A claim of general applicability of the current method cannot be made. The method will probably be useful in clean sandstones and in sandstones that do not have fine materials located in pore throats. It should be noted that fines migration has been observed in regional Turonian well flow tests. Fine material is obviously present as evidenced by some of the derived pore throat size distribution curves and the SEM image shown in Figure 12. However, these fines do not appear to affect the routine measurement of permeability. Its applicability to carbonate reservoirs is an open question. However, the success experienced in the current reservoir should encourage further investigation. Finally, in the present tests, the MIP tests were performed without overburden while

other tests were performed with a net overburden. Permeability is known to be sensitive to confining stress; the effect of this difference in test procedure is not known.

CONCLUSIONS

The present work, which is based on the pioneering work of Purcell, has provided a simple method for deriving a predictive equation for calculating the permeability of rock from MIP and electrical properties data. This method has been shown to be extremely accurate for samples from an offshore oil and gas condensate field in Ghana. This success was in spite of the fact that the data set was not originally designed with the present work in mind. A protocol has been provided for the application of this method to any field. Future application will reveal if this method has general applicability to reservoir calculations.

ACKNOWLEDGMENTS

The authors thank Tullow Oil Ghana and its partners for permission to publish these results. Douglas Ruth's work is supported by the Natural Science and Engineering Research Council of Canada.

REFERENCES

1. Ritter and Drake, "Pore-Size Distribution in Porous Materials", I&EC-Analytical Edition, Vol. 17, No. 12, pp. 782-786, 1945.
2. Leverett, M.C., "Capillary Behaviour in Porous Solids", *AIME Transactions*, (TP 1223), Vol. 142, pp. 152-168, 1941.
3. Purcell, W.R., "Capillary Pressures – Their Measurement using Mercury and the Calculation of Permeability Therefrom", *AIME Transactions*, (TP 2544), Vol. 186, pp. 39-48, 1949.
4. Thomeer, J.H.M. , "Introduction of a Pore Geometrical Factor Defined by the Capillary Pressure Curve", *AIME Transactions*, (TN 2057), Vol. 219, pp. 354-358, 1960.
5. Swanson, B.F., "A Simple Correlation between Permeabilities and Mercury Injection Capillary Pressures", *JPT*, Vol. 33, No. 12, pp. 2498-2504, 1981.

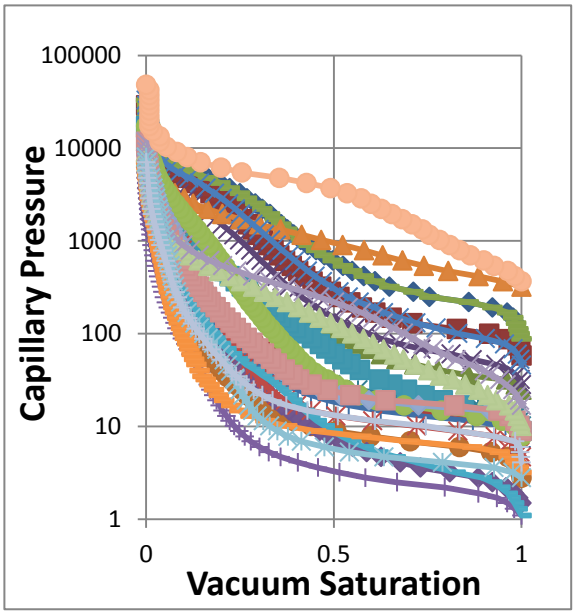

Figure 2 The original mercury injection capillary pressure curves.

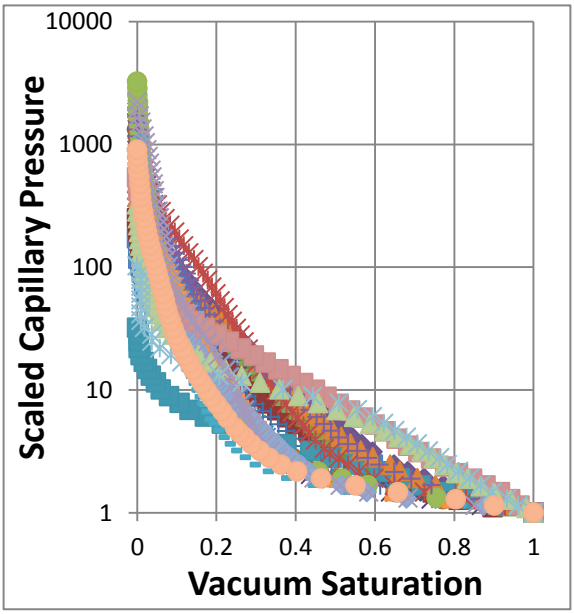

Figure 3 The mercury injection curves corrected for surface pore invasion.

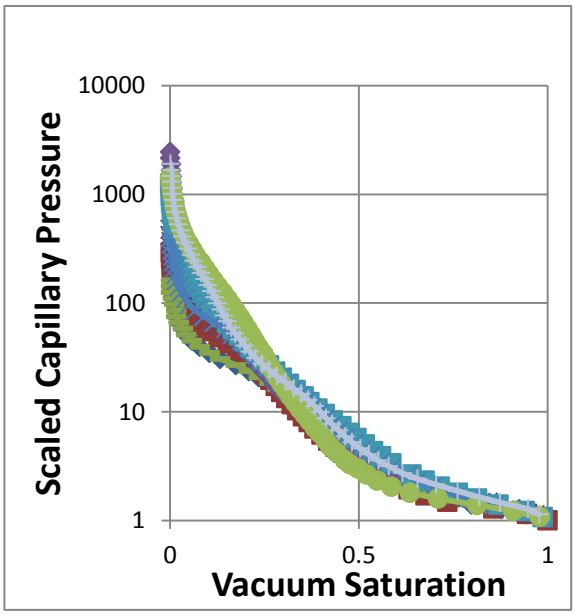

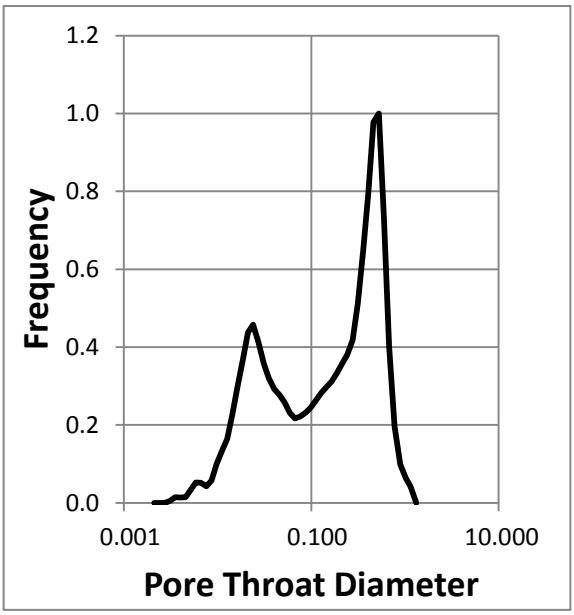

Figure 4 Curves of the bi-modal pore throat size distribution type. The left figure shows the collection of curves. The right figure shows a representative pore throat size distribution curve.

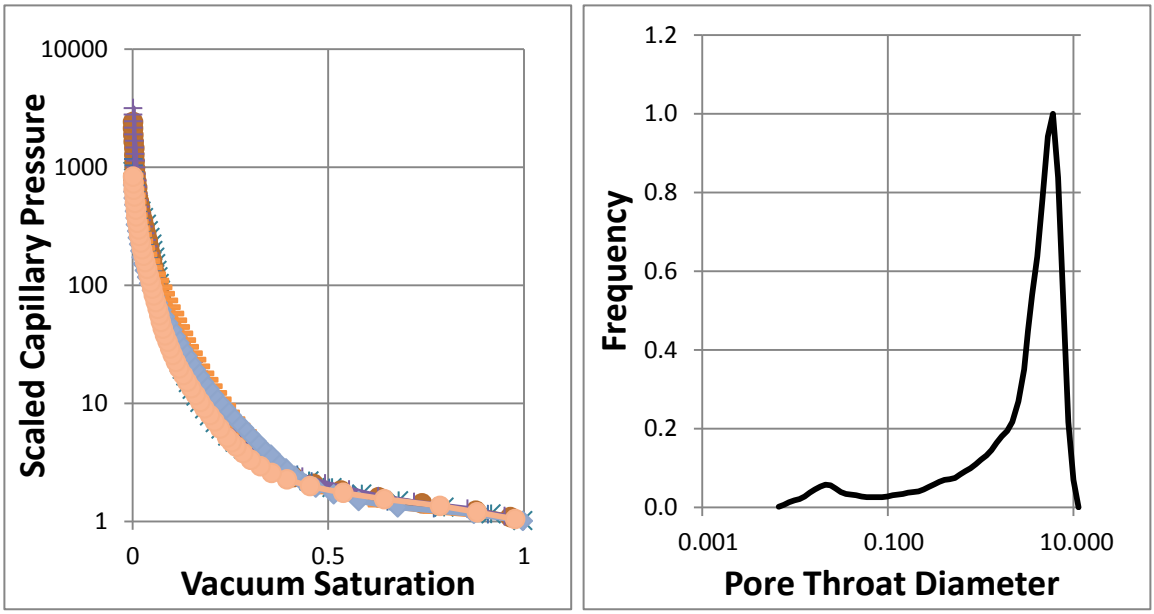

Figure 5 Curves of the uni-modal pore throat size distribution type. The left figure shows the collection of curves. The right figure shows a representative pore throat size distribution curve.

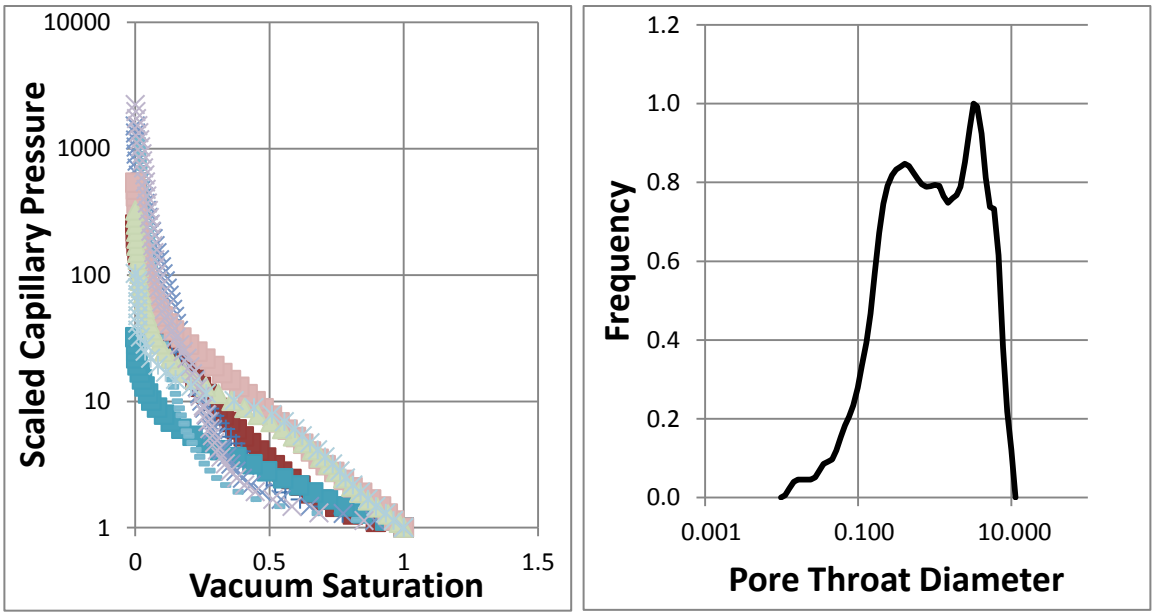

Figure 6 The remaining curves. The left figure shows the collection of curves. The right figure shows one of a variety of pore throat size distribution curves.